Manuscript prepared for Atmos. Meas. Tech. Discuss.
with version 2014/07/29 7.12 Copernicus papers of the LaTeX class copernicus.cls.
Date: 5 June 2015

Calibration and instrumental line shape characterisation of a set of portable FTIR spectrometers for detecting greenhouse gas emissions

M. Frey[1], F. Hase[1], T. Blumenstock[1], J. Groß[1], M. Kiel[1], G. Mengistu Tsidu[1,3], K. Schäfer[2], M. K. Sha[1], and J. Orphal[1]

[1]Karlsruhe Institute of Technology (KIT), Institute for Meteorology and Climate Research (IMK-ASF), Karlsruhe, Germany
[2]Karlsruhe Institute of Technology (KIT), Institute for Meteorology and Climate Research (IMK-IFU), Garmisch-Partenkirchen, Germany
[3]Department of Physics, Addis Ababa University, P.O. Box 1176, Addis Ababa, Ethiopia

Correspondence to: M. Frey (m.frey@kit.edu)

Abstract

A comprehensive calibration procedure for mobile, low-resolution, solar-absorption FTIR spectrometers, used for greenhouse gases observations, is developed. These instruments commend themselves for campaign use. The instrumental line shape (ILS) of each spectrometer has been thoroughly characterised by analysing the shape of H_2O signatures in open path spectra. A setup for the external source is suggested and the invariance of derived ILS parameters with regard to chosen path length is demonstrated. The instrumental line shape characteristics of all spectrometers were found to be close to nominal. Side-by-side solar observations before and after a campaign, which involved shipping of all spectrometers to a selected target site and back, are applied for verifying the temporal invariability of instrumental characteristics and for deriving intercalibration factors for $X\mathrm{CO}_2$ and $X\mathrm{CH}_4$, which take into account residual differences of instrumental characteristics. An excellent level of agreement and stability was found between the different spectrometers: the uncorrected biases in $X\mathrm{CO}_2$ and $X\mathrm{CH}_4$ are smaller than 0.01 and 0.15 %, respectively, and the drifts are smaller than 0.005 and 0.035 %. As an additional sensitive demonstration of the instrumental performance we show the excellent agreement of ground pressure values obtained from the total column measurements of O_2 and barometric records. We find a calibration factor of 0.9700 for the spectroscopic measurements in comparison to the barometric records and a very small scatter between the individual spectrometers (0.02 %). As a final calibration step, using a co-located TCCON spectrometer as a reference, a common scaling factor has been derived for the $X\mathrm{CO}_2$ and $X\mathrm{CH}_4$ products derived from the low-resolution spectrometers, which ensures that the records are traceable to the WMO in situ scale.

1 Introduction

The continuing increase of atmospheric greenhouse gas abundances is the major driver of anthropogenic global warming. Accurate measurements of the variable atmospheric con-

centrations are required for the quantification of sinks and sources of these gases (Olsen and Randerson, 2004). Recently great efforts have been undertaken to measure column-averaged dry air mole fractions of greenhouse gases with global coverage. Examples are satellite-borne instruments like SCIAMACHY (Frankenberg et al., 2006), GOSAT (Morino et al., 2011) or the recently launched OCO-2 sensor (Frankenberg et al., 2015). For the validation of OCO-2, a network of ground based high resolution Fourier-transform infrared (FTIR) spectrometers of the type 125HR from Bruker has been initiated by the California Institute of Technology: the Total Carbon Column Observation Network (TCCON). Currently, about 23 TCCON globally distributed stations measure the column-averaged abundances of greenhouse gases in the atmosphere, by recording solar absorption spectra in the near infrared (NIR) (Wunch et al., 2010). TCCON has been carefully calibrated against in situ aircraft measurements and sets the reference for remote-sensing measurements of column-averaged greenhouse gas observations. However, it is difficult to use this technical approach for the observation of sources and sinks on a regional scale, because the laboratory spectrometers applied for TCCON are not portable. Recently, KIT developed, in cooperation with Bruker, Ettlingen, a portable low resolution FTIR spectrometer for the observation of greenhouse gases in the NIR and demonstrated the excellent stability of the device (Gisi et al., 2012). The spectrometer is now available from Bruker under the part name EM27/SUN. This lightweight device has low infrastructure demands so it can be operated on a campaign basis, at remote places and even on mobile platforms such as ships (Klappenbach et al., 2015). These features not only enable the EM27/SUN to contribute to the total column measurements of the TCCON in previously underrepresented regions, in particular it can be used to gain additional information about isolated sinks and sources of greenhouse gases. Boundary layer abundances of greenhouse gases influenced by emissions from cities have been observed since long using mass spectroscopic (von der Weiden-Reinmüller et al., 2014) or cavity ring down techniques e.g. (Newman et al., 2013; Rella et al., 2013). The downside of this approach is the high sensitivity to local sources, which overemphasizes the near vicinity, and the sensitivity with respect to assumptions on vertical exchange of air masses.

An alternative approach is the application of ground based remote sensing application. This kind of method has been applied for the quantification of localized sources, e.g. refineries (Mellqvist et al., 2010), power plants (Utembe et al., 2014), and large cities (Wunch et al., 2009; Wong et al., 2015). Hase et al. (2015) demonstrate a sophisticated approach to measure the emissions of a mega city: five EM27/SUN spectrometers were operated along the circumference of the Berlin metropolitan area. Over a period of three weeks, column averaged dry air mole fractions of $X\mathrm{CH_4}$ and $X\mathrm{CO_2}$ have been observed simultaneously at all stations. The emission of Berlin introduces an increase of downwind column averaged mole fractions in the sub percentage range. Therefore, high precision and stability of the instruments are a prerequisite of this approach. In this work, we develop a calibration scheme allowing for a reliable detection of small source signals from a differential analysis using data collected by several portable spectrometers. We hope that the proposed methods will contribute to the definition of a good practice for ensuring the reliability of data collected with portable, low-resolution FTIR spectrometers for campaigns as well as possible network applications. We constructed a suitable external radiation source and performed lab-air observations of water vapor signatures for the determination of instrumental line shape (ILS) characteristics. Moreover, we tested the spectrometers used in Berlin side-by-side for several days before and after the campaign, determined the level of instrumental stability and deduced calibration factors for $X\mathrm{CH_4}$ and $X\mathrm{CO_2}$ in order to assure that data measured by different spectrometers are compatible among each other and with TCCON measurements.

2 Instrumentation and spectrometer characteristics

2.1 EM 27 SUN spectrometer

For the acquisition of solar spectra we utilize the Bruker EM27/SUN which was developed in collaboration with the KIT. A detailed description of the spectrometer can be found in Gisi

et al. (2012), in the following only a short overview including changes from the original setup is given.

The EM27/SUN features a RockSolid^{TM} pendulum interferometer with two cube corner mirrors and a CaF_2 beamsplitter. This setup achieves high stability against thermal influences and vibrations. Gimbal-mounted retroreflectors move a geometrical distance of 0.45 cm leading to an optical path difference (OPD) of 1.8 cm which corresponds to a spectral resolution of 0.5 cm^{-1}. As a minor modification of the prototype spectrometer described by Gisi et al. (2012), the production device contains an off-axis mirror with a focal length of 127 mm for centering the solar beam on the detector. Together with the field stop (0.6 mm diameter) this leads to a semi Field-of-View (FOV) of 2.36 mrad which results in an external FOV of about 56 % of the apparent solar disc diameter. Measurements are recorded with an InGaAs detector operated at ambient temperature. Due to an electronics update it is now possible to record double-sided interferograms of 0.5 cm^{-1} resolution. The detector is a photodiode type G12181-010K from Hamamatsu with a size of 1 mm $\times$ 1 mm and spectral coverage from 5000 to 11 000 cm^{-1}. In contrast to the detector used in the prototype that operated in the spectral region between 6000 and 9000 cm^{-1}, the wider spectral coverage allows the observation of CH_4. In addition, total columns of O_2, CO_2 and H_2O are derived from the recorded spectra. The detector signal is DC coupled and thereby supports the correction of variable atmospheric transmission (Keppel-Aleks et al., 2007).

2.2 Ghost to parent ratio

The EM 27 records spectra in the region from 100 to 15 798 cm^{-1}, so in order to satisfy the Nyquist theorem the sampling of the interferogram has to be performed at every zerocrossing of the laser signal (HeNe laser, wavelength 633 nm). If the signal is not taken at exactly zero intensity, systematic sampling errors are introduced leading to artefacts in the measured spectrum, so called sampling ghosts (Messerschmidt et al., 2010; Dohe et al., 2013). The manufacturer has recently released an effective workaround for this problem which we adopted for our measurements. A temporal linear interpolation is applied for locating the downward zero crossings. This method suppresses the ghosts below the detection limit

($< 5 \times 10^{-6}$). In addition, we tested this set up for possible line shape errors and other kinds of out-of-band artefacts, but found no detrimental effects.

2.3 Intrumental line shape

Precise knowledge of a spectrometer's instrumental line shape (ILS) is of utmost importance to gain correct information from measurements because using wrong ILS values leads to systematic errors in the gas retrieval. The ILS can be divided into two parts. One part describes the modulation loss through inherent self-apodization of the spectrometer which is present also in an ideal instrument. This contribution can easily be calculated utilizing the OPD and FOV of the spectrometer. The other component of the ILS results from misalignments and optical aberrations of the spectrometer and can be characterised by a modulation efficiency amplitude and a phase error, both functions of the OPD (Hase et al., 1999). These parameters have to be deduced from lab measurements.

Here we implement an ILS characterisation scheme for the EM27/SUN. Whereas for TCCON spectrometers the standard procedure to derive the ILS are gas cell measurements, our proposed approach uses an open-path observation of a few meters of lab air to avoid the need for a gas cell, only an external light source is needed. The ILS is derived from H_2O lines in the 7000 and 7400 cm^{-1} spectral region. The selected microwindow encompasses a large number of water vapour lines spanning a wide range of line intensities. Residuals of spectral fits to fully resolved open path spectra collected with the TCCON spectrometer were used to verify that the selected microwindow does not contain lines with significantly inconsistent line parameters.

Fig. 1 shows a picture of our lamp system. We employ an Osram Halogen 50 W lamp as radiation source, together with a fast aspherical collimation lens of 2 inches diameter, as used in projection collimators. In order to avoid channeling we tilted the light bulb with respect to the optical axis, and for assuring a uniform illumination the glass surface of the bulb is roughened towards the lens by use of a piece of sandpaper. The system is mounted on a stable, height-adjustable tripod because this much alleviates the fine adjustment for achieving a uniform light beam on the tracker mirror and a uniform image of the source on

the field stop. Due to the modification of the bulb a voltage lower than the nominal voltage should be applied for operation. A stabilized digital laboratory DC power supply is used, we apply 11 V voltage. Two hours prior to the actual measurements the instrument should be powered up to guarantee that the unstabilized reference laser operates at a constant wavelength. As the water column inside the spectrometer can not be neglected, we recommend to vent the instrument by opening the two apertures of the spectrometer, in order to ensure that the mixing ratio of water vapor is about the same inside and outside the spectrometer. The apertures are opened when the instrument is switched on and closed after recording of the spectra. As we depend on stable thermal conditions and because we temporarily violate the sealed spectrometer closure, we recommend to apply this procedure only in a reasonably clean, controlled environment. It is mandatory not to open the spectrometer apertures if the instrument is colder than the surrounding because of the risk of condensation or if the humidity in the room is too high. The distance between instrument and lamp should not be chosen too small, because otherwise the heat of the lamp will affect a non-negligible section of the open path, thus introducing a systematic error. Furthermore care should be taken that the free aperture of the tracker is fully illuminated and that the image of the lamp on the field stop is evenly illuminated and exceeds the diameter of the field stop. This can be achieved by shifting and tilting the source and by rotating the mirrors of the solar tracker using its internal camera. The resulting illumination on the field stop aperture can also be comfortably judged using this camera. For the measurements itself we propose to record 30 times 10 double-sided scans at full resolution. The settings in the measurement file are the same as for solar measurements except that we use the highest pregain setting. We obtain the final spectrum used in the subsequent analysis by taking the averaged interferogram, performing a DC-correction and a Fourier transformation. In order to predict the correct width of the observed H_2O lines and so correctly retrieve the ILS width, the distance between instrument, measured from the first tracking mirror, and lamp needs to be measured as well as air temperature and pressure at the time of measurement. In our setup, temperature and pressure were recorded using a Lutron MHB-382SD data logger with a temperature accuracy of $\pm 0.8\,^{\circ}\mathrm{C}$ and pressure accuracy of $\pm 3\,\mathrm{hPa}$ (above 1000 hPa) or $\pm 2\,\mathrm{hPa}$ (be-

low 1000 hPa). The optical path length between first tracking mirror and the longpass filter (38 cm) is fixed as well as the path length inside the spectrometer housing (58 cm). These contributions have to be added to the aforementioned distance. For the analysis of the measured data we use version 14 of the retrieval software LINEFIT (Hase et al., 1999). As the ILS characteristics were close to nominal, we used the simple two-parameter ILS model. For the H_2O linelist we use the HITRAN 2009 linelist with minor adjustments, see Sect. 4.1. A preliminary LINEFIT analysis run on the measured spectrum is performed in order to determine the H_2O column. From this H_2O column value, the total path length, and the temperature, the partial pressure of H_2O is calculated. This value is afterwards used for the final LINEFIT run, which provides the ILS parameters. A typical fit result is shown in Fig. 2. The standard deviation of the residual is $1\sigma = 0.24\,\%$. For providing a demonstration of the level of reliability of the procedure, we determined ILS parameters from spectra recorded at several different distances. The results are depicted in Fig. 3, applying two different ways of performing the analysis. The simple analysis assumes a uniform path between lamp and detector. The more refined approach divides the observed absorption into two contributions, one from inside and one from outside the spectrometer. We assume that due to the venting, the mixing ratio of H_2O inside the spectrometer is the same as outside, but we respect that the air inside the spectrometer is slightly warmer due to power dissipation of the spectrometer. Temperature inside the spectrometer is recorded by a sensor provided in the housekeeping data of each OPUS file. As indicated by Fig. 3, both results are in agreement within 0.15%. We recommend to follow the refined procedure which is probably more accurate. Note that the deduced ILS parameters are also quite consistent as function of distance between source and spectrometer.

We measured the ILS for the different spectrometers before and after the Berlin campaign. The resulting ILS values are presented in Table 1. For the trace gas retrieval we use the mean value of the measurements before and after the campaign, the setup for these experiments was exactly the same. The values show very good agreement. The correlation between modulation efficiency amplitude and XCO_2 was deduced from a sensitivity test. We ran PROFFIT retrievals for one hour of measurements during noon assuming different

ILS values with otherwise unchanged parameters. A change of 1 % in the modulation efficiency led to a change of 0.15 % in XCO_2. This is in agreement with Gisi et al. (2012). Intrument 2 has the biggest difference in terms of ILS modulation efficiency before and after the campaign with 0.24 %, corresponding to a change of only 0.04 % for the column-averaged dry-air mole fraction (DMF) of carbon dioxide, XCO_2. Note that this is not self-evident since the instruments were transported from Karlsruhe to Berlin by road, thus experiencing a lot of mechanical impacts and vibrations.

3 Measurement sites and data acquisition

In order to measure small differences upstream and downstream of a source, the instrument to instrument consistency is of utmost importance to avoid bias between stations. For this purpose, calibration measurements were carried out.

3.1 Calibration measurements at KIT Campus North

The calibration measurements were performed before the Berlin campaign on three sunny days between 6 June and 16 June 2014 and after the campaign on three consecutive days 16–18 July 2014 on top of our office building north of Karlsruhe, with an altitude of 133 m a.s.l., coordinates are 49.094° N and 8.434° E. The spectrometers were moved from the lab on the fourth floor to the roof terrace on the seventh floor thus being exposed to mechanical stress. Then they were coarsely oriented north, without effort for levelling. If further orientation was needed, we manually moved the spectrometer so that the solar beam was centered onto the entrance window. The CamTracker program was then able to track the sun. As we operated the EM27/SUN in summer, it was heated up to temperatures above 40 °C. In order to protect the electronics from the heat, we built a sun cover for the EM27/SUN, which reduced the temperatures inside the spectrometer by about 10 °C. We recorded double-sided interferograms with 0.5 cm^{-1} resolution. With 10 scans and a scanner velocity of 10 kHz, one measurement takes about 58 s. For precise time recording, we used a GPS Receiver. Additionally, on-site pres-

sure and temperature profiles are available from tall tower meteorological measurements (http://imkbemu.physik.uni-karlsruhe.de/~fzkmast/).

4 Data analysis

4.1 Data processing

In a first step, the recorded interferograms are Fourier transformed using the Norton-Beer-Medium apodisation function. This apodisation is useful for reducing sibelobes around the spectral lines, an undesired feature in unapodised low resolution spectra, which would complicate the further analysis. Furthermore, a DC-correction is performed. Together with a quality filter, which discards interferograms with intensity fluctuations above 10 % and intensities below 10 % of the maximal modulation amplitude, this is implemented in a Python tool. In this work, we analyzed spectra utilizing the PROFFIT Version 9.6. This code is in wide use and has been thoroughly tested in the past, e.g. (Schneider and Hase, 2009; Schneider et al., 2010; Sepúlveda et al., 2012). Due to the low resolution of the EM27/SUN, we fitted the atmospheric spectra by scaling of a-priori trace gas profiles. As source of the a-priori profiles, we utilized the WACCM ver. 6 climatology (http://www2.cesm.ucar.edu/working-groups/wawg). For the retrieval we need accurate temperature and pressure profiles. In case of the Karlsruhe calibration experiments we use on-site data together with MERRA model data, which provides temperature and pressure data on a $1.25° \times 1.25°$ grid from 1000 to 0.1 hPa 8 times a day. Every retrieval depends on the choice of linelists for the solar lines and atmospheric gases absorption lines. We use the HITRAN 2008 line list in its original form for CH_4, the HITRAN 2008 linelist with a line-mixing parameterisation for CO_2 adopted from a code provided by Lamouroux et al. (2010) and the linelist used by TCCON for O_2. For the H_2O linelist we use the HITRAN 2009 linelist with changes used by (Wunch et al., 2010) and additional ad hoc adjustments where it seemed appropriate.

4.2 Spectral windows

For the evaluation of the O_2 gas column we use the 7765–8005 cm^{-1} spectral region, which is also applied in the TCCON analysis (Wunch et al., 2010). For CO_2 we combine the spectral windows used by TCCON to one larger window ranging from 6173 to 6390 cm^{-1}. CH_4 is evaluated in the 5897–6145 cm^{-1} spectral domain. For H_2O the 8353 to 8463 cm^{-1} region is used. An example fit for the different spectral windows is shown in Fig. 4. The residual of the spectral fit for the water column retrieval is much bigger than for the other gases because of the difficulties in measuring H_2O line parameters. The standard deviation of the residual is $\sigma = 0.2\,\%$ for CO_2 and CH_4, $\sigma = 0.1\,\%$ for O_2 and $\sigma = 0.5\,\%$ for H_2O.

5 Calibration measurement results

In this section we present results of the calibration measurements performed before and after the Berlin campaign. First we show the uncalibrated total columns followed by column-averaged DMF $X\mathrm{Gas}$ of carbon dioxide and methane, where $X\mathrm{Gas}$ is defined as

$$X\mathrm{Gas} = \frac{\mathrm{Gas}_{\mathrm{Column}}}{\mathrm{O2}_{\mathrm{Column}}} \cdot 0.2095 \tag{1}$$

To make the measurements comparable to WMO scale, in TCCON the standard procedure is to divide the calculated DMFs by a calibration factor (Wunch et al., 2010). The application of this TCCON calibration factor is also an inherent part of our post processing. For $X\mathrm{CO}_2$ the factor is 0.9898 whereas it is 0.9765 for $X\mathrm{CH}_4$.

5.1 Total column amounts

In Fig. 5 are depicted the column values of the measured species of the different instruments. It is clear that the lineshape of all the spectrometers is nearly identical. Data gaps appearing for all instruments were caused by passing clouds. In addition Instrument 4 suffered from a hardware problem on June, 13, 2014 as well as on two days after

the Berlin campaign and therefore was only partly able to perform measurements. The tracker of this instrument did not follow the sun anymore but moved to a random position during initialization. This was caused by a mechanical problem of the azimuthal tracker motor. Intraday changes of the O_2 column can be mostly attributed to pressure changes, which will be shown in Sect. 5.2. There are slight systematic offsets, strongest between Instrument 2 and Instrument 4 with a difference of 0.2 %. However, note that a similar offset is also observed in the CO_2 and CH_4 gas columns, as can be seen in Fig. 5, therefore the resulting effects on the target quantities $X\mathrm{CO}_2$ and $X\mathrm{CH}_4$ are much smaller. For a better comparison an intercalibration factor between the instruments is established. This is done in the following way. We take the separate measurement days and divide the data into smaller bins of 15 min duration. Inside each bin all available values are averaged. This quantity is used as a reference value. For each individual station, the difference between each value and its bin reference is calculated. The squared sum of all these residuals sets the cost function contribution of the station. The total cost function is given by the sum of all station contributions. In an iterative procedure, the scaling factors for all stations are adjusted for minimizing the total cost function while the side constraint of an invariant average value of all scaling factors is respected (We neglect the fact that the number of values per bin is slightly variable - in a more rigorous approach, an individual statistical weight of each bin could be taken into account when the associated contributions to the cost function is calculated). In Table 2 the calibration factors for the O_2 column for the calibration measurements before and after the campaign are given. Differences before and after the campaign are very small, only 0.04 % for Instrument 2 and 4 and even less for the other instruments. This is suprisingly good, because column values are sensitive to various potential error sources, including ILS errors, timing errors, tracking errors and nonlinearities.

5.2 O_2 column as an indicator of instrumental stability

The consistency between retrieved O_2 and measured surface pressure is a very sensitive test for the instrumental stability because for the oxygen column, there is no compensation

of possible instrumental problems which were discussed in the previous section. In order to compare the dataset with barometer measurements recorded at the ground level of the Karlsruhe meteorological tall tower, we calculate the ground pressure from the measured O_2 and H_2O total columns:

$$P_S = (O_{2\text{Column}} \div 0.2095 \times \bar{\mu} + H_2O_{\text{Column}} \times \mu_{H_2O}) \times g \times \exp\left(-\frac{\Delta h}{h_S}\right) \quad (2)$$

P_S is the surface pressure, $\bar{\mu}$ the molecular mass of dry air, μ_{H_2O} the molecular mass of water, g the gravity acceleration, Δh the height difference between the Karlsruhe tall tower ground level and the Institute terrace where the EM27/SUN spectrometers were located and h_S the scaling height. We find a systematic scaling factor of 0.9700 between these records and the barometric ground pressure. This factor was calculated with the method described in the previous section and is in good agreement with other observations (Hase et al., 2015) or (Klappenbach et al., 2015). Its origin can mainly be attributed to oxygen line intensity errors (Washenfelder et al., 2006). The scatter between the different instruments is smaller than 0.02 %. In Fig. 6 we scaled the pressure values obtained from the total columns to the barometric data for better comparability. The record of the dry ground pressure is compatible with the retrieved water vapor and molecular oxygen column.

5.3 Column-averaged dry air mole fraction

Figure 7 shows the column-averaged DMF of CO_2, which was calculated using Eq. (1). In this representation systematic errors tend to cancel out, which leads to a high degree of reproducibility in the time series difference between the instruments. Until this point, no post calibration has been performed, only the individual ILS of each instrument has been taken into account. Table 3 shows the intercalibration factor for XCO_2 and XCH_4 before and after the campaign. The method to derive the factors is the same that was used for the O_2 column calibration. For XCO_2 we obtain an agreement within the measured noise level. The difference is below 0.005 % or 0.02 ppm for all instruments. This means we can apply a global intercalibration factor which is valid before and after the campaign. This is

an important prerequisite for campaign measurements. For $X\mathrm{CH_4}$ the agreement is slightly worse at 0.035 %, but still very good. In Fig. 8 the calibrated $X\mathrm{CH_4}$ time series for the calibration measurements is depicted. Note that one global intercalibration factor is applied for all measurement days. The scatter is very low for both species. Variations during the day stem from real signals, for example the $X\mathrm{CO_2}$ peaks on July, 16, 2014 were also measured by a co-located TCCON instrument (see Fig. 9).

5.4 Solar zenith angle dependency

There is a slight solar zenith angle (SZA) dependency in the $X\mathrm{CO_2}$ and $X\mathrm{CH_4}$ data, which is hard to see in Figs. 7 and 8 because the SZA is small during a considerable fraction of the day in summer, and the temporal variability of the target gases is superimposed to the SZA dependence. In order to make the data compatible with the WMO reference scale, it is nevertheless important to correct for a systematic airmass dependency originating from spectroscopic uncertainties and approximations by the radiative transfer model. For this we use a method similar to that implemented by Wunch et al. (2010) in TCCON. The correction formula is

$$X\mathrm{Gas_c} = X\mathrm{Gas_{unc}} \left\{ 1 + a \left[\left(\frac{\theta + b}{90^\circ + b} \right)^2 - \left(\frac{45^\circ + b}{90^\circ + b} \right)^2 \right] \right\}$$

where a, b are fit parameters, θ is the SZA, $X\mathrm{Gas_c}$ and $X\mathrm{Gas_{unc}}$ are the airmass dependency corrected and uncorrected column-averaged DMF of the respective species. The choice of 45° as the neutral angle is arbitrary and does not influence the fit results. For the determination of the correction parameters we do not use our calibration measurement data recorded in Karlsruhe. The dataset it is not well suited for this task due to the actual intraday variability which occured. Instead we use parameters obtained from a comprehensive evaluation of EM27/SUN data from a ship cruise (Klappenbach et al., 2015). These data are not influenced by local source contributions and clearly show the SZA dependency in the $X\mathrm{CO_2}$ and $X\mathrm{CH_4}$ data. For these measurements the $\mathrm{O_2}$ column-averaged mole fraction does not show a detectable SZA dependence for SZA $< 80^\circ$; the SZA dependence is essentially

generated by the CO_2 and CH_4 mole fractions in the numerator. The obtained parameters are $a = 6.296 \times 10^{-3}$, $b = 1.291$ for XCO_2 and $a = 3.796 \times 10^{-3}$, $b = 16.04$ for XCH_4. Using this correction we receive data comparable to in situ scale measurements, supported by the comparison with a collocated TCCON spectrometer. Figure 9 shows the airmass dependency corrected XCO_2 values together with TCCON DMF for 16 July. Additionally an in situ scaling was performed to match the EM27/SUN values to the TCCON instrument. This factor of 0.9951 was determined with the method described in Sect. 5.1. The EM27/Sun values match the TCCON values remarkably well. Note that due to the much lower spectral resolution of the EM27/SUN, the noise level of the resulting XCO_2 data is even smaller as compared to the data generated by the TCCON spectrometer. Again one global factor was found valid for the measurements before and after the campaign. Figure 10 shows XCH_4 values for the same day. Similar to XCO_2 the values between EM27/SUN spectrometers and TCCON instrument differ slightly towards evening. For the in situ scaling factor we obtain 0.9951.

6 Conclusions

In this work we implemented an extensive calibration routine for mobile, low-resolution FTIR spectrometers. The instruments, used for greenhouse gases observations, are particularly suited for campaign use and for operation at remote places because of their compact design. A method for the accurate characterisation of the instrumental line shape from open path measurements was presented. The ILS characteristics were found to be close to nominal for all spectrometers, the temporal variability is small. The drifts between the instruments, which were shipped for a campaign and back between the measurements, are smaller than 0.24 % modulation efficiency amplitude at maximum optical path difference. In order to verify the temporal invariability of the instrumental characteristics and to derive intercalibration factors for XCO_2 and XCH_4, side-by-side solar observations were carried out. The drifts are smaller than 0.005 % and 0.035 %, respectively, the uncorrected biases are smaller than 0.01 % and 0.15 %. As an additional sensitive test of the instrumental sta-

bility we show a comparison of ground pressure values obtained from barometric records and from the total column measurements of O_2. A scaling factor of 0.9700 was found between the different techniques. Scatter of the instruments is 0.02 %. Furthermore an empirical airmass correction was applied to compensate for a spurious SZA dependency of the data. Finally, by a comparsion with a co-located TCCON instrument, we derived a common calibration factor of 0.9951 ± 0.0001 valid for both XCO_2 and XCH_4 making the records traceable to the WMO in situ scale. Because of the high level of stability of the spectrometers demonstrated in this work, we are confident that our routine allows the unambiguous detection of XCO_2 enhancements in the sub-ppm range for CO_2 and ppb range for CH_4. We conclude that this approach can be used for the detection of local sinks and sources of various kinds.

Acknowledgements. We acknowledge support by the ACROSS research infrastructure of the Helmholtz Association.

We acknowledge Friedrich Klappenbach from the "Institute for Meteorology and Climate Research – Atmospheric Trace Gases and Remote Sensing (IMK-ASF)" at the KIT for providing the fit parameters used for the correction of the SZA dependency.

We acknowledge Stephan Kraut from the "Institute for Meteorology and Climate Research – Troposphere Research (IMK-TRO)" at the KIT for providing tall-tower meteorological data.

We acknowledge the Global Modelling and Assimilation Office (GMAO) and the GES DISC for the dissemination of Merra meteorological datasets.

We acknowledge Michael Gisi and Gregor Surawicz from Bruker for their invaluable support in bringing the EM27/SUN spectrometers into service.

The article processing charges for this open-access publication have been covered by a Research Centre of the Helmholtz Association.

References

Dohe, S., Sherlock, V., Hase, F., Gisi, M., Robinson, J., Sepúlveda, E., Schneider, M., and Blumenstock, T.: A method to correct sampling ghosts in historic near-infrared Fourier transform

spectrometer (FTS) measurements, Atmos. Meas. Tech., 6, 1981–1992, doi:10.5194/amt-6-1981-2013, 2013.

Frankenberg, C., Meirink, J. F., Bergamaschi, P., Goede, A. P. H., Heimann, M., Körner, S., Platt, U., van Weele, M., and Wagner, T.: Satellite chartography of atmospheric methane from SCIAMACHY on board ENVISAT: Analysis of the years 2003 and 2004, J. Geophys. Res., 111, D07303, doi:10.1029/2005JD006235, 2006.

Frankenberg, C., Pollock, R., Lee, R. A. M., Rosenberg, R., Blavier, J.-F., Crisp, D., O'Dell, C. W., Osterman, G. B., Roehl, C., Wennberg, P. O., and Wunch, D.: The Orbiting Carbon Observatory (OCO-2): spectrometer performance evaluation using pre-launch direct sun measurements, Atmos. Meas. Tech., 8, 301–313, doi:10.5194/amt-8-301-2015, 2015.

Gisi, M., Hase, F., Dohe, S., Blumenstock, T., Simon, A., and Keens, A.: XCO_2-measurements with a tabletop FTS using solar absorption spectroscopy, Atmos. Meas. Tech., 5, 2969–2980, doi:10.5194/amt-5-2969-2012, 2012.

Hase, F., Blumenstock, T., and Paton-Walsh, C.: Analysis of the instrumental line shape of high-resolution Fourier transform IR spectrometers with gas cell measurements and new retrieval software, Appl. Optics, 38, 3417–3422, doi:10.1364/AO.38.003417, 1999.

Hase, F., Frey, M., Blumenstock, T., Groß, J., Kiel, M., Kohlhepp, R., Mengistu Tsidu, G., Schäfer, K., Sha, M. K., and Orphal, J.: Use of portable FTIR spectrometers for detecting greenhouse gas emissions of the megacity Berlin – Part 2: Observed time series of XCO_2 and XCH_4, Atmos. Meas. Tech. Discuss., doi:10.5194/amt-8-2767-2015, 2015.

Keppel-Aleks, G., Toon, G. C., Wennberg, P. O., and Deutscher, N. M.: Reducing the impact of source brightness fluctuations on spectra obtained by Fourier-transform spectrometry, Appl. Optics, 46, 4774–4779, doi:10.1364/AO.46.004774, 2007.

Klappenbach, F., Bertleff, M., Kostinek, J., Hase, F, Blumenstock, T., Agusti-Panareda, A., Razinger, M., and Butz, A.: Accurate mobile remote sensing of XCO_2 and XCH_4 latitudinal transects from aboard a research vessel, AMT, submitted, 2015.

Lamouroux, J., Tran, H., Laraia, A., Gamache, R., Rothman, L., Gordon, I., and Hartmann, J.-M.: Updated database plus software for line-mixing in CO_2 infrared spectra and their test using laboratory spectra in the 1.5–2.3 µm region, J. Quant. Spect. Radiat. T., 111, 2321–2331, doi:10.1016/j.jqsrt.2010.03.006, 2010.

Mellqvist, J., Samuelsson, J., Johansson, J., Rivera, C., Lefer, B., Alvarez, S., and Jolly, J.: Measurements of industrial emissions of alkenes in Texas using the solar occultation flux method, J. Geophys. Res.-Atmos., 115, D00F17, doi:10.1029/2008JD011682, 2010.

Messerschmidt, J., Macatangay, R., Notholt, J., Petri, C., Warneke, T., and Weinzierl, C.: Side by side measurements of CO_2 by ground-based Fourier transform spectrometry (FTS), Tellus B, 62, 749–758, doi:10.1111/j.1600-0889.2010.00491.x, 2010.

Morino, I., Uchino, O., Inoue, M., Yoshida, Y., Yokota, T., Wennberg, P. O., Toon, G. C., Wunch, D., Roehl, C. M., Notholt, J., Warneke, T., Messerschmidt, J., Griffith, D. W. T., Deutscher, N. M., Sherlock, V., Connor, B., Robinson, J., Sussmann, R., and Rettinger, M.: Preliminary validation of column-averaged volume mixing ratios of carbon dioxide and methane retrieved from GOSAT short-wavelength infrared spectra, Atmos. Meas. Tech., 4, 1061–1076, doi:10.5194/amt-4-1061-2011, 2011.

Newman, S., Jeong, S., Fischer, M. L., Xu, X., Haman, C. L., Lefer, B., Alvarez, S., Rappenglueck, B., Kort, E. A., Andrews, A. E., Peischl, J., Gurney, K. R., Miller, C. E., and Yung, Y. L.: Diurnal tracking of anthropogenic CO_2 emissions in the Los Angeles basin megacity during spring 2010, Atmos. Chem. Phys., 13, 4359–4372, doi:10.5194/acp-13-4359-2013, 2013.

Olsen, S. C. and Randerson, J. T.: Differences between surface and column atmospheric CO2 and implications for carbon cycle research, J. Geophys. Res.-Atmos., 109, D02301, doi:10.1029/2003JD003968, 2004.

Rella, C. W. and Chen, H. and Andrews, A. E. and Filges, A. and Gerbig, C. and Hatakka, J. and Karion, A. and Miles, N. L. and Richardson, S. J. and Steinbacher, M. and Sweeney, C. and Wastine, B. and Zellweger, C.: High accuracy measurements of dry mole fractions of carbon dioxide and methane in humid air, Atmospheric Measurement Techniques, 6, 837–860, doi:10.5194/amt-6-837-2013, 2013.

Schneider, M. and Hase, F.: Ground-based FTIR water vapour profile analyses, Atmos. Meas. Tech., 2, 609–619, doi:10.5194/amt-2-609-2009, 2009.

Schneider, M., Sepúlveda, E., García, O., Hase, F., and Blumenstock, T.: Remote sensing of water vapour profiles in the framework of the Total Carbon Column Observing Network (TCCON), Atmos. Meas. Tech., 3, 1785–1795, doi:10.5194/amt-3-1785-2010, 2010.

Sepúlveda, E., Schneider, M., Hase, F., García, O. E., Gomez-Pelaez, A., Dohe, S., Blumenstock, T., and Guerra, J. C.: Long-term validation of tropospheric column-averaged CH_4 mole fractions obtained by mid-infrared ground-based FTIR spectrometry, Atmos. Meas. Tech., 5, 1425–1441, doi:10.5194/amt-5-1425-2012, 2012.

Utembe, S. R. and Jones, N. and Rayner, P. J. and Genkova, I. and Griffith, D. W. T. and O'Brien, D. M. and Lunney, C. and Clark, A. J.: Estimating CO_2 emissions from point sources: a case study

of an isolated power station, Atmospheric Chemistry and Physics Discussions, 14, 31551–31601, doi:10.5194/acpd-14-31551-2014, 2014.

von der Weiden-Reinmüller, S.-L., Drewnick, F., Zhang, Q. J., Freutel, F., Beekmann, M., and Borrmann, S.: Megacity emission plume characteristics in summer and winter investigated by mobile aerosol and trace gas measurements: the Paris metropolitan area, Atmos. Chem. Phys., 14, 12931–12950, doi:10.5194/acp-14-12931-2014, 2014.

Washenfelder, R. A., Toon, G. C., Blavier, J.-F., Yang, Z., Allen, N. T., Wennberg, P. O., Vay, S. A., Matross, D. M., and Daube, B. C.: Carbon dioxide column abundances at the Wisconsin Tall Tower site, J. Geophys. Res.-Atmos., 111, D22305, doi:10.1029/2006JD007154, 2006.

Wong, K.W., Fu, D., Pongetti, T.J., Newman, S., Kort, E.A., Duren, R., Hsu, Y.-K., Miller, C.E., Yung, Y. L. and Sander, S.P.: Mapping CH_4 : CO_2 ratios in Los Angeles with CLARS-FTS from Mount Wilson, California, Atmos. Chem. Phys., 15, 241 – 252, doi:10.5194/acp-15-241-2015, 2015.

Wunch, D., Weenberg, P.O., Toon, G.O., Keppel-Aleks, G., and Yavin, Y.G.: Emissions of greenhouse gases from a North American megacity, Geophysical Research Letters, 36, L15810, doi:10.1029/2009GL039825, 2009.

Wunch, D., Toon, G. C., Wennberg, P. O., Wofsy, S. C., Stephens, B. B., Fischer, M. L., Uchino, O., Abshire, J. B., Bernath, P., Biraud, S. C., Blavier, J.-F. L., Boone, C., Bowman, K. P., Browell, E. V., Campos, T., Connor, B. J., Daube, B. C., Deutscher, N. M., Diao, M., Elkins, J. W., Gerbig, C., Gottlieb, E., Griffith, D. W. T., Hurst, D. F., Jiménez, R., Keppel-Aleks, G., Kort, E. A., Macatangay, R., Machida, T., Matsueda, H., Moore, F., Morino, I., Park, S., Robinson, J., Roehl, C. M., Sawa, Y., Sherlock, V., Sweeney, C., Tanaka, T., and Zondlo, M. A.: Calibration of the Total Carbon Column Observing Network using aircraft profile data, Atmos. Meas. Tech., 3, 1351–1362, doi:10.5194/amt-3-1351-2010, 2010.

Table 1. Compilation of ILS modulation efficiencies measured at maximum OPD = 1.8 cm. Measurements were performed in Karlsruhe in June and July 2014, in between the spectrometers were transported for campaign measurements by road thus experiencing a lot of mechanical impacts and vibrations.

Instr.	3 Jun	15 Jul
1	0.9979	0.9996
2	0.9914	0.9938
3	0.9971	0.9997
4	1.0010	1.0020
5	0.9959	0.9963

Table 2. Calibration factors for O_2 column for the different instruments. Measurements were performed in June and July 2014, in between the spectrometers were transported for campaign measurements. Instrument 1 has been scaled to one, which is an arbitrary choice.

Instr.	O_2 col. June	O_2 col. July
1	1.0000	1.0000
2	1.0001	0.9997
3	1.0004	1.0002
4	1.0024	1.0020
5	1.0012	1.0011

Table 3. Calibration factor for $X\mathrm{CO}_2$ and $X\mathrm{CH}_4$ for the different instruments. Measurements were performed in Karlsruhe June and July 2014, in between the spectrometers were transported for campaign measurements.

Instr.	$X\mathrm{CO}_2$ June	$X\mathrm{CO}_2$ July	$X\mathrm{CH}_4$ June	$X\mathrm{CH}_4$ July
1	1.00000	1.00000	1.00000	1.00000
2	0.99924	0.99921	0.99927	0.99940
3	1.00015	1.00016	0.99971	0.99962
4	0.99987	0.99987	0.99856	0.99882
5	0.99960	0.99962	0.99892	0.99905

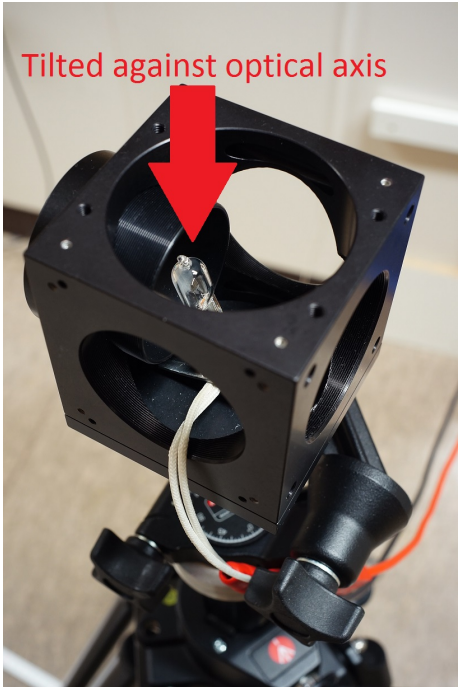

Figure 1. Setup of the lamp system. The bulb is tilted against the optical axis to avoid channeling. The lamp system is mounted on a height-adjustable tripod for the fine adjustment of the light beam.

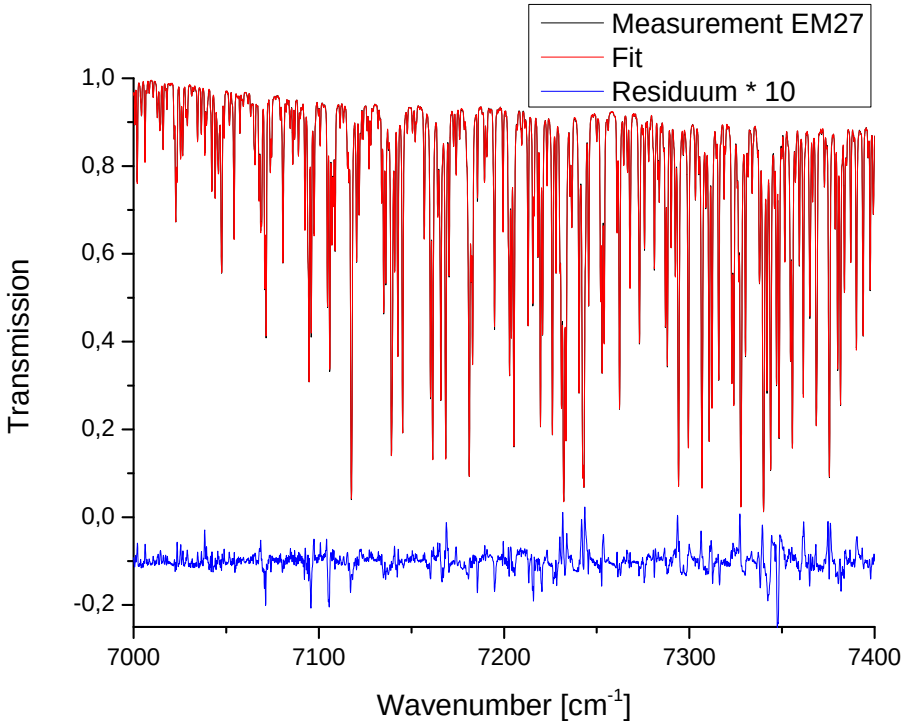

Figure 2. Transmission spectrum of 4 m lab air (black curve) in the 7000 to 7400 cm^{-1} region. Overlying is the LINEFIT calculation (red curve), the residuum multiplied by a factor of ten is shown in blue. For clarity reasons, an offset of -0.1 was added to the residuum.

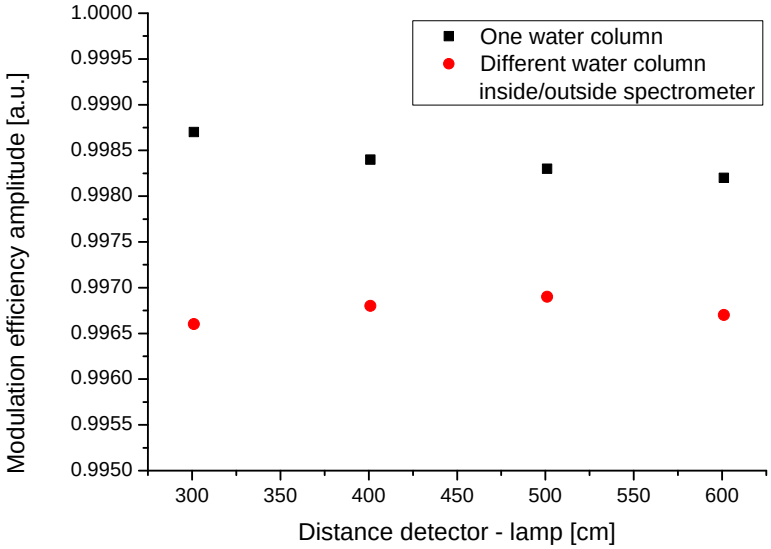

Figure 3. ILS results obtained with LINEFIT for two different ways of performing the analysis. The simple analysis assumes a uniform path between lamp and detector, whereas the more refined approach divides the observed absorption into one contribution from inside and one from outside the spectrometer. Results are in agreement within 0.15%.

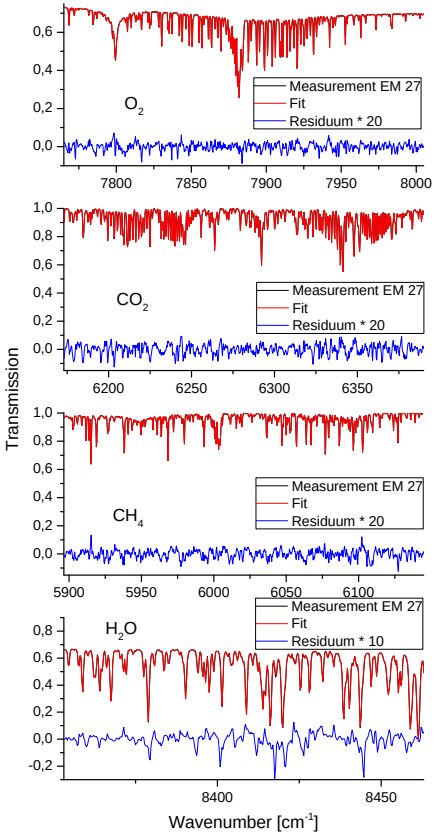

Figure 4. Spectral windows used during the retrieval for the different species. The fit is in accordance with the measurement, the residuum, which has been multiplied with a factor of 10 for H_2O and 20 for the other species, is small.

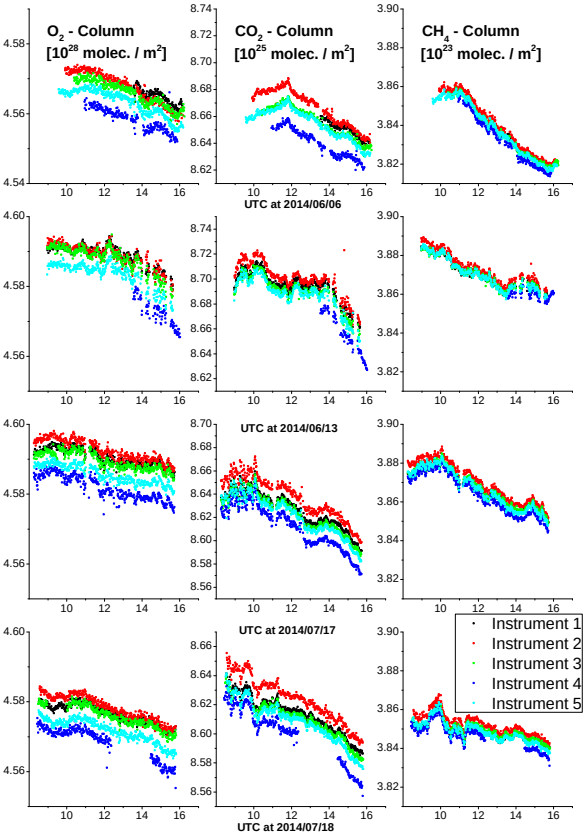

Figure 5. Total columns of O_2, CO_2 and CH_4 for the different spectrometers on four days of the calibration measurements in Karlsruhe. Solar observations were performed in June and July 2014, in between the spectrometers were transported for campaign measurements. One data point consists of 10 interferograms, the measurement time being 58 s each.

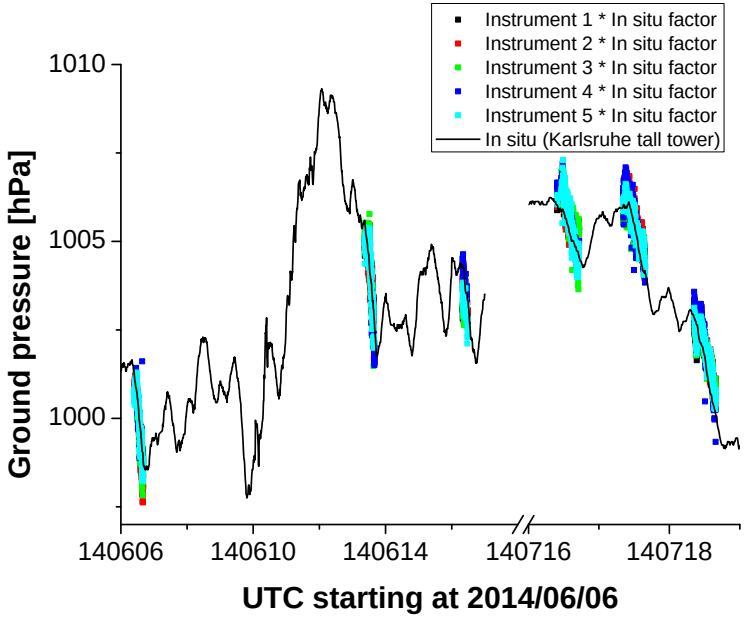

Figure 6. In situ pressure data from the Karlsruhe tall tower (http://imkbemu.physik.uni-karlsruhe.de/~fzkmast/) together with pressure data calculated from total column amounts of O_2 and H_2O. The column data is scaled with an in situ factor of 0.9700 for better comparability.

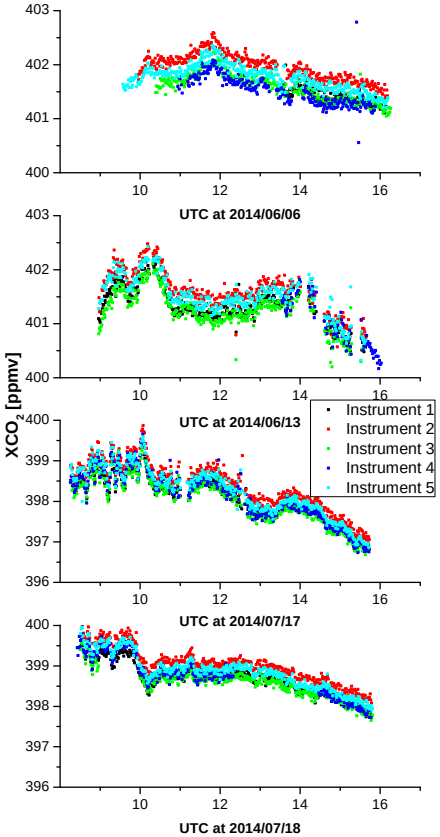

Figure 7. Uncalibrated XCO_2 values for all instruments. Experiments and measurement days are the same as for O_2.

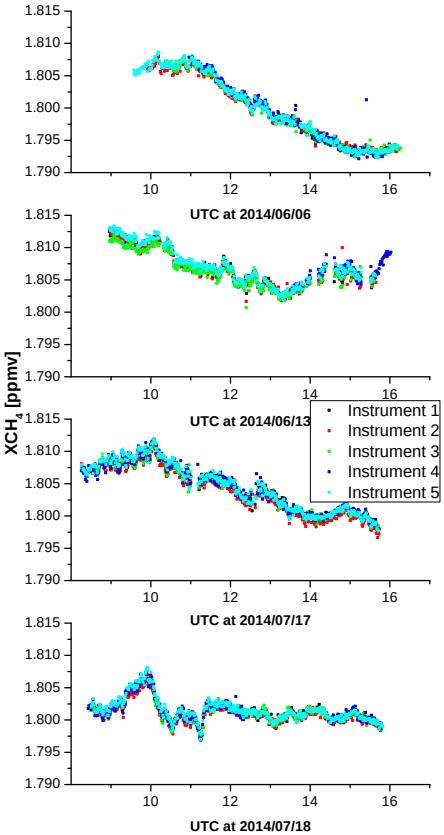

Figure 8. Calibrated XCH_4 values for all instruments. Experiments and measurement days are the same as for O_2.

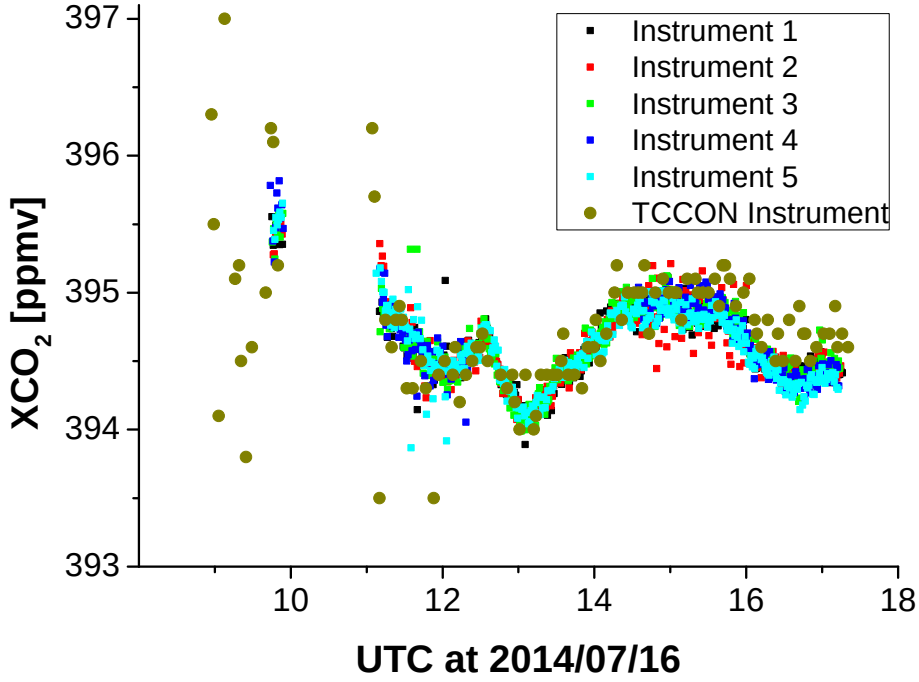

Figure 9. Calibrated and SZA corrected XCO_2 values for all EM27/SUN spectrometers on 16 July. Golden dots show XCO_2 data from a co-located TCCON instrument.

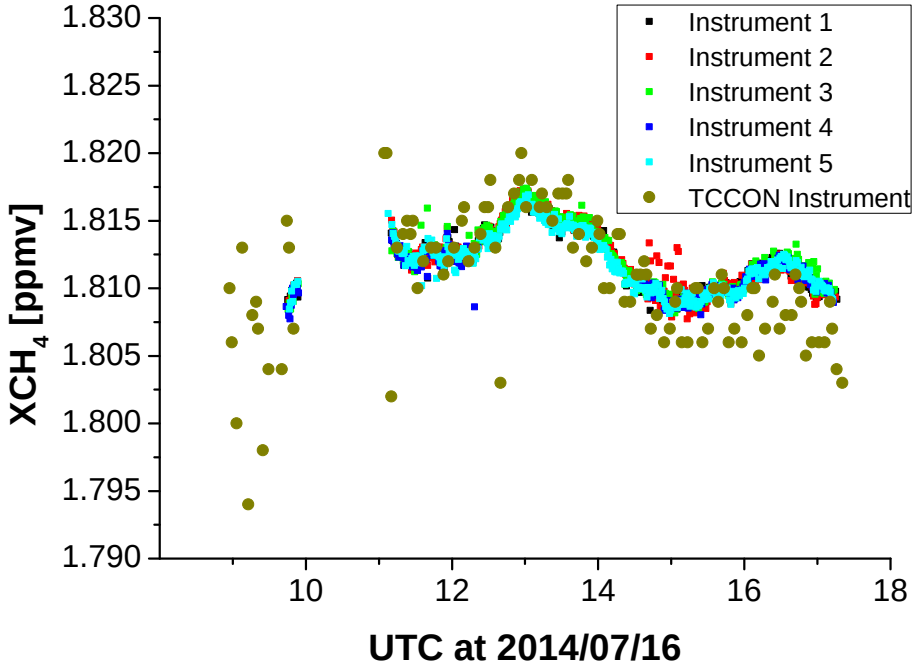

Figure 10. Calibrated and SZA corrected XCH_4 values for all EM27/SUN spectrometers on 16 July. Golden dots show XCH_4 data from a co-located TCCON instrument.